

# Simulation of lithospheric-plate collision by using DEM. Example of the Arabian platform motion.

Jean-François Parrot<sup>1</sup> and Bernard Collet<sup>2</sup>

<sup>1</sup> LAGE, Instituto de Geografía, Universidad Nacional Autónoma de México [UNAM], Mexico.

<sup>2</sup> GAEL Consultant, 25 rue Alfred Nobel, 77420 Champs sur Marne, France  
 Email: [parrot@igg.unam.mx](mailto:parrot@igg.unam.mx); [jfparrot@hotmail.com](mailto:jfparrot@hotmail.com); [bernard.collet@gael.fr](mailto:bernard.collet@gael.fr)

**ABSTRACT** A high resolution Digital Elevation Model (DEM) is used to simulate and quantify the consequence of lithospheric-plate confrontation. The algorithm takes into account the calculated mountainous chain and the reconstitutions of the original formation steps.

The procedure consists in applying to the DEM a mask composed of two different limits, namely i) a fixed and ii) a moving limit (see figure). The moving limit is displaced in an iterative way, until reaching the initial position of the punching plate.

The extrapolation of the altitude values on a given transect takes into account i) the initial distance  $D_{in}$  between the limits before moving, ii) the distance  $D_{out}$  between the fixed limit and the new position of the moving limit, and iii) the original altitude of the points encountered in the transect. On the other hand, two regions are located outside of the mask. The region located upstream on the transect remains unchanged, as the downstream region is moved according the moving limit motion, but without any modification of their altitude values. The DEM can be rotated in such a way that transects follow the columns, from the fixed to the moving limit. For this case, the algorithm inside the mask can be simplified, where  $i$  is the unique variable employed. If  $i_{start} < i < i_{end\_in}$  then the altitude value ( $A_{out}$ ) and the location ( $i', j$ ) of the pixel corresponding to the transformation are obtained from equations 7, 8 and 11 in the text.

$$A_{out}^{i=i_{start}, i_{end\_in}}(i', j) = \left[ A_{min} + \left( A_{in}(i, j) - A_{min} / R \right) \right] \quad (7)$$

$j = j_{start}, j_{end\_in}$

$i' = i + [(i - i_{start}) \times R]$  and  $j' = j$  (8) with  $R = D_{out} / D_{in}$ ,  $D_{in} = i_{end\_in} - i_{start}$ ,  $D_{out} = D_{in} + St$ .  $St$  and  $MaxD$  correspond to the step and the maximum displacement defined by the user, respectively.

The computation of the altitude  $A_{out}(i', j')$  requires defining the minimum altitude value  $A_{min}$  of each studied transect. Comparing the altitude of the transect starting point  $A_{in}(i_{start}, j_{start})$  and the altitude  $A_{in}$  at the point  $(i_{end\_in}, j_{end\_in})$ ,  $A_{min}$  corresponds to the lower altitude value.

In the presence of a punching point (see Fig. 4), the computation of elongation follows the formulas (7) and (8), yet the stretching applied to each transect depends on the value of  $D_{out}$  calculated as follows:  $D_{out} = D_{in} + St'$  where  $St' = St \times (D_{min} / D_{in})$  and  $D_{min}$  is the distance in front of the punching point.

As the motion of the pushing plate is directly related to the  $St$  value, the algorithm generates an empty space assumed to correspond to the old oceanic crust.

DEM's simulations generating mountainous chains allow quantifying the displacement of material during an orogenesis, while reconstituting the surface occupied by the chain before its formation. Therefore DEM's allow determining with a high degree of precision plate boundaries before collision, and consequently to assess the shortening rate. Finally DEM's allow modelling in a continuous way the collision effects and considering orogenic evolution with time.

In the case of Eastern Turkey, the total displacement is equal to 210 km and we asses that the rate motion of the Arabian plate stands between 10.5 mm/year and 8.9 mm/year if the movement started at the beginning of Miocene (20 or 23.5 millions years).

**Keywords:** DEM simulation, Lithospheric-plate collision, Arabian platform motion.

## INTRODUCTION

DEM's simulations generating mountainous chains allow quantifying the displacement of material during an orogenesis, reconstituting the surface occupied by the chain before its formation, hence, determining with more precision the plate boundaries before a collision and therefore assessing the shortening rate, and finally modelling in a continuous way the collision effects and so looking for the evolution of the orogenesis during time.

We developed in such a goal the present algorithm, in the frame of a geo-structural survey of oriental Turkey, but we estimated that this procedure could be presented from a merely methodological point of view, because this technique seems applicable in many cases of collision.

## DESCRIPTION OF THE METHOD

### General algorithm:

Data\_in correspond to a raster DEM where the altitude value  $z$  is a function of  $x, y$  (coordinates of each surface point). This value  $z = f(x, y)$  is reported in an image file either in integer (2 bytes or 4 bytes) or with a decimal value (4 or 8 bytes).

The zone that is submitted to the linear expansion is defined as a binary image, the size of which corresponds to the DEM size. This zone that plays the role of a mask can be drawn using the shadowed DEM and it is recorded with the value 1, the background being equal to 0. In order to avoid border effects, the zone has generally to be drawn in such a way that it crosses the whole image. The mask is characterized by two different limits defining three regions. The first one corresponds to a fixed limit; the second one is a moving limit (Fig. 1). This last limit is moved in an iterative way, until reaching the position defined by the user.

On the other hand, two regions are located out of the mask. The upstream region remains unchanged, and the downstream region is moved according to the second limit motion, without any modification of its altitude values.

When the coordinates  $(i, j)$  of a pixel located on a transect are in the mask, in other words, when this pixel is located between the coordinates  $(i_{start}, j_{start})$  corresponding to the intersection of the transect with the fixed limit and the coordinates  $(i_{end\_in}, j_{end\_in})$  that correspond to the intersection of the transect with the moving limit before starting, the values of  $i_{end\_in}$  and  $j_{end\_in}$  are researched in an

iterative way until reaching the border of the mask. The successive values of  $i''$  and  $j''$  are equal to:

$$i'' = i + (n \times \sin \alpha_{tr}) \text{ and } j'' = j + (n \times \cos \alpha_{tr}) \quad (1)$$

$n$  is regularly incremented according to a given step (i.e. 0.2).

When the border of the mask is reached, then  $i_{end\_in} = i''$  and  $j_{end\_in} = j''$ .

$$i_{start} \leq i \leq i_{end\_in} \text{ and } j_{start} \leq j \leq j_{end\_in}$$

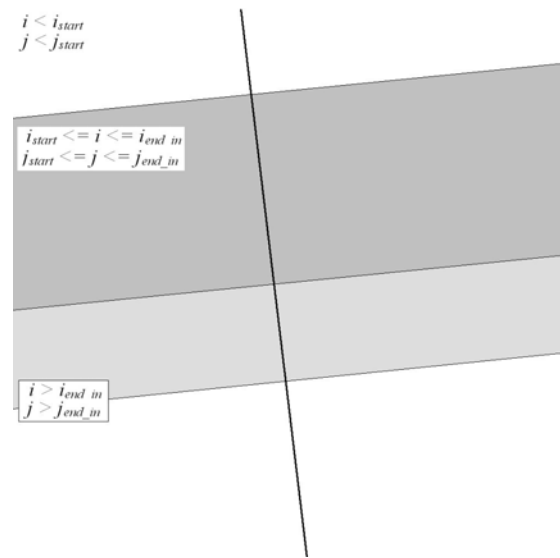


Figure 1 General scheme.

As the geological orientation is defined in relation to the North (value  $0^\circ$ ) and taking into account a clockwise rotation, the angle  $\alpha$  of orientation defined by the user, has to be replaced in the trigonometric space. The trigonometric value of  $\alpha_{tr}$  is equal to:  $\alpha_{tr} = 90^\circ - \alpha$ .

It then becomes possible to calculate the distance  $D_{in}$  of the transect inside the mask and the distance  $D_{out}$  of its corresponding elongated transect, assuming that the step displacement  $St$  follows the same orientation and corresponds to a constant.

On the other hand, the elongation ratio  $R$  is equal to:  $R = D_{out}/D_{in}$  and the coordinates of  $i_{end\_out}$  and  $j_{end\_out}$  are respectively equal to:

$$D_{in} = \sqrt{(i_{end\_in} - i_{start})^2 + (j_{end\_in} - j_{start})^2} \quad (3)$$

$$D_{out} = D_{in} + St \quad (4)$$

Parrot and Collet, Simulation of lithospheric-plate collision by using DEM. Example of the Arabian platform motion.

$$i_{end\_out} = i_{start} + \lfloor (i_{end\_in} - i_{start}) \times R \rfloor \quad (5)$$

$$j_{end\_out} = j_{start} + \lfloor (j_{end\_in} - j_{start}) \times R \rfloor \quad (6)$$

$St$  corresponds to the step displacement defined by the user up to a maximum displacement ( $MaxD$ ) also given by the user. In order to follow the behaviour of the DEM during the perpendicular elongation of the mountainous range,  $St$  can be incremented until  $MaxD$  during the process.

Then the altitude value ( $A_{out}$ ) and the location ( $i'$ ,  $j'$ ) of the pixel corresponding to the transformation are respectively equal to: (equations 7 and 8)

$$A_{out}^{i=i_{start}, j=j_{start}; i=i_{end\_in}, j=j_{end\_in}}(i', j') = [A_{min} + ((A_{in}(i, j) - A_{min}) / R)]$$

$$\text{with } i' = i + \lfloor (i - i_{start}) \times R \rfloor \text{ and } j' = j + \lfloor (j - j_{start}) \times R \rfloor$$

The computation of the altitude  $A_{out}(i', j')$  requires defining the minimum altitude value  $A_{min}$  of each studied transect. Comparing the altitude  $A_{in}(i_{start}, j_{start})$  of the transect starting point and the altitude  $A_{in}(i_{end\_in}, j_{end\_in})$  of the transect ending,  $A_{min}$  corresponds to the lower altitude value.

If the former condition ( $i_{start} \leq i \leq i_{end\_in}$  and  $j_{start} \leq j \leq j_{end\_in}$ ) is not encountered, that is to say when the studied pixel is located outside of the mask, two different possibilities arise.

a) first case:

The pixel is located on a linear segment which is upstream from the mask when following transect. The altitude value and the position of the pixel remain unchanged:

$$A_{out}(i', j') = A_{in}(i, j), \text{ with } i' = i \text{ and } j' = j. \quad (9)$$

b) second case:

The pixel is located on a linear segment which stands downstream from the mask when following the transect.

In this case, if the altitude value is not changed, its position ( $i'$ ,  $j'$ ) undergoes a displacement as previously calculated.

### Simplified algorithm

Actually, a displacement that does not follow the lines or the columns gives rise to border effects and a loss of information can be registered (i.e. a

45° orientation generates around 25% of uncertainties); furthermore when computing the displacement, the ( $i'$ ,  $j'$ ) position resulting from the resample in the raster mode, introduces a bias that increases when iterating.

Thus, in order to avoid these handicaps, the studied DEM is replaced in such a way, that transects run following the columns, from the upper part to the lower one. In this case, the algorithm can be simplified, as  $i$  is the unique variable employed.

When, for each column, the value of  $i$  (following the lines) is kept between  $i_{start}$  and  $i_{end\_in}$ , the altitude value ( $A_{out}$ ) and the location ( $i'$ ,  $j$ ) of the pixel corresponding to the hypsometric conversion are respectively equal to:

$$A_{out}^{i=i_{start}, j=j_{start}; i=i_{end\_in}, j=j_{end\_in}}(i', j) = [A_{min} + ((A_{in}(i, j) - A_{min}) / R)] \quad (10)$$

$$\text{with } i' = i + \lfloor (i - i_{start}) \times R \rfloor$$

$$R = D_{out} / D_{in}, D_{in} = i_{end\_in} - i_{start} \text{ and } D_{out} = D_{in} + St \quad (11)$$

$St$  and  $MaxD$  correspond respectively to the step and the maximum displacement defined by the user (see above).

$A_{min}$  and  $A_{out}$  are calculated as formerly described.

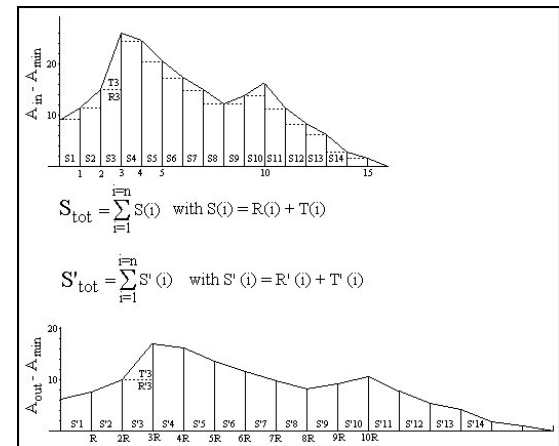


Figure 2 Surface calculations.

In fact, some ( $i$ ,  $j$ ) positions of the stretched transect remain without corresponding altitude values, and a secondary interpolation is needed to obtain a complete transect. But this last treatment introduces a light global loss of material. For this

reason, we developed another approach allowing to calculate and to compare the initial transect surface and the surface of the stretched transect (Fig. 2). The calculated deviation cannot exceed  $\pm 0.5\%$  of  $S_{tot}$ ; elsewhere it is necessary to slightly and temporarily modify the value of the parameter  $R$  used to compute locally the altitude points of the incorrect stretched transect until satisfying the former condition.

The successive values of  $A_{out}$  and the values resulting from the  $R$  increment are reported in a provisory table in order to finally transfer to the pixels describing the elongated transect their corresponding values of altitude (Fig. 3).

2) outside the mask

Outside the mask the computation follows the same condition as explained in the case of the general algorithm.

### Punching algorithm

The computation of elongation is conducted as described above; it is related to the ratio existing between the reference cross-section located in front of the punching point. The algorithm searches either directly on the mask the minimum length distance  $D_{min}$  and then the coordinate of the column, or this coordinate is defined by the user and  $D_{min}$  is calculated further.

Then in the mask, the computation follows the formulas (c) and (d), but the elongation applied to each column depends on the value of  $D_{out}$  (Fig. 4).

$$D_{out} = D_{in} + St' \text{ where } St' = St \times (D_{min} / D_{in}) \quad (12)$$

Since the motion of the pushing plate is directly related to the  $St$  value, the algorithm generates an empty space corresponding to the old oceanic crust.

A more precise calculation requires estimating the role of the erosion during the motion time; to this end we must assume that the original relief was higher than in present time. On the other hand, the volume of removed material according to the erosion rate must be calculated in order to reconstitute the original transect profile before erosion. For these reasons, we need to calculate for each transect point the thickness of the eroded material during time  $T_M$ . The volume of eroded material depends on the local erosion rate  $\tau_{LOC}$  according to the slope and the regional erosion rate  $\tau$  ( $m^3/km^2/y$ ) value.

The time  $T_M$  corresponding to a lithospheric-plate displacement depends on the plate velocity  $P_V$  (defined in meter for year). This time is equal to:  $T_M = (St \times P_S) / P_V$ , where  $St$  corresponds to the step (number of pixels) and  $P_S$  to the pixel size (in meters).

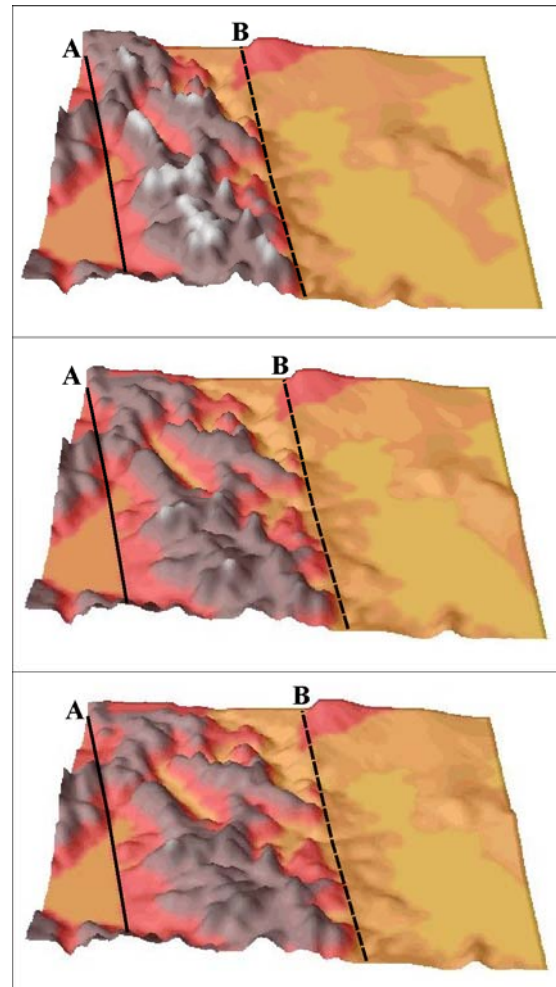


Figure 3 Example of mountain stretching. A corresponds to the fixed limit and B to the moving limit.

The estimation of the erosion rate  $\tau$  generally depends on the nature of the geological material, the climatic conditions, the slope value, etc. For instance  $\tau$  can be considered as a function of drainage area  $A$  and local slope  $S$ ,  $\tau = \kappa A^m S^n$  where  $\kappa$  is a constant that incorporates climatic factors and rock vulnerability,  $m$  and  $n$  varying with the different erosion processes. Other approaches can be used to determine the material failure in a caption area (Wilson and Gallant, 2000) and then to define erosion rates.

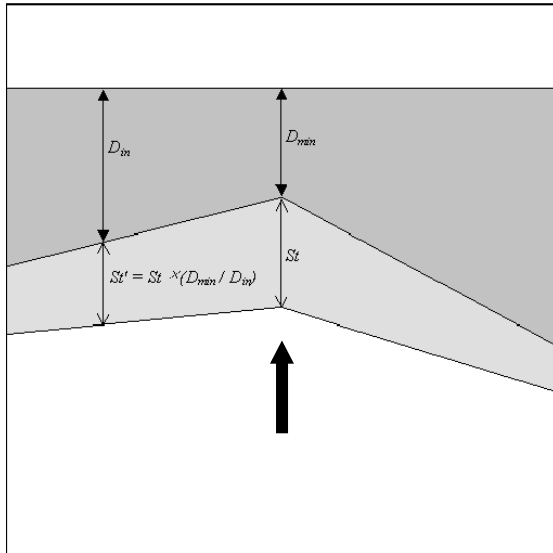


Figure 4 Displacement observed when applying the punching algorithm.

Actually, estimation of erosion rate may vary from  $5 \text{ m}^3/\text{km}^2/\text{year}$  (Gao et al., 2002; Calixto-Albarran and Parrot, 2007),  $80$  (Lee et al, 1999),  $250$  (Watson and Evans, 1991), until  $900 \text{ m}^3/\text{km}^2/\text{year}$  (Bartsch et al, 2002) or even more.

Without entering in to more details, we assume that the local erosion rate for each DEM point is equal to:  $\tau_{LOC} = [\xi \tau \times \sigma^2] - [(10\xi \times \tau) \times \sigma]$  where  $\sigma$  is the slope value and  $\xi$  a coefficient equal to  $0.000139$ ; i.e. for  $\tau = 20$ ,  $y = 0.00278 x^2 - 0.0278 x$  and for  $\tau = 100$ ,  $y = 0.0139 x^2 - 0.139 x$  (Fig. 5).

The local thickness  $\theta_{LOC}$  at the time  $T_M = 0$  is equal to  $\theta_{LOC} = \tau_{LOC} / 1000^2$  and the total thickness  $\theta_{(i,j)}$  of the studied point is equal to  $\theta_{(i,j)} = \theta_{LOC} \times T_M$

Our results show that the low grade of the pixel resolution ( $500 \times 500$  meters) blurs the slope values. Less than 6% of the studied region registers slopes higher or equal to  $30^\circ$  and the mean value is equal to  $14^\circ$  in such a way that the erosion rate remains at the global scale lower than it can be normally expected. Nevertheless we can assess that based on slope values, erosion rate retained and duration time, the thickness of the material removed by runoff erosion and landslides can be as high as 8 or 9 meters, but values approximate 1 meter. In this light, using a 500 meters DEM, these values are not sufficient enough to modify the results provided by the simulation.

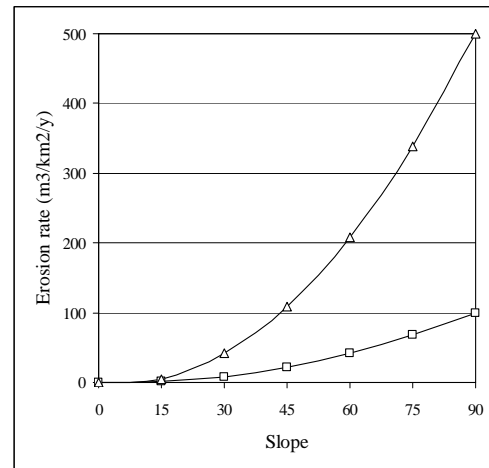


Figure 5 Relationships slope / erosion rates.

## APPLICATION

The capacity of plate tectonic concepts to describe horizontal motions remains questionable (Thatcher, 2003) and gave rise to opposite interpretations. Some authors (Tapponnier et al., 1982; Peltzer and Saucier, 1996; Peltzer and Tapponnier, 1998), propose that the deformation of the continental lithosphere corresponds to a mosaic of rigid lithospheric blocks bounded by fast-slipping faults. In this regard, deformation would be then driven exclusively by boundary forces due for example to the India-Eurasia collision. Others (England and Houseman, 1986; Houseman and England, 1993) propose that deformation is omnipresent and continents can be treated as a continuously deforming viscous medium where faults play a minor role.

The treatment developed in the present paper and applied to Eastern Turkey is related with this last concept. Geological history of Turkey is poorly understood, partly because of the problem of how the region has been tectonically assembled by plate motions and because reconstructing the ensemble needs to ensure the collage of different pieces of ancient continental and oceanic lithosphere joined together by younger igneous, volcanic and sedimentary rocks.

The studied region is part of the great Alpine belt that extends from the Atlantic Ocean to the Himalaya Mountains. This belt was formed during the Tertiary Period as the Arabian, African, and Indian continental plates began to collide with the Eurasian Plate and this process is still at work today as the African Plate converges with the Eurasian Plate and the Anatolian Plate escapes

Parrot and Collet, Simulation of lithospheric-plate collision by using DEM. Example of the Arabian platform motion.

towards the west and southwest along strike-slip faults (Fig. 6).

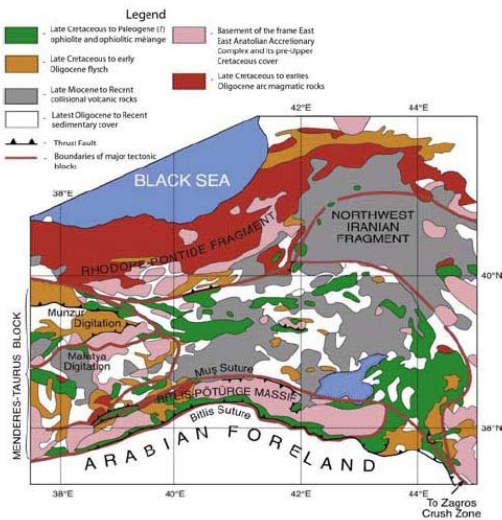


Figure 6 Geological sketch map of the studied region (Sengor et al., 2003).

The two main values of the aspect (E and W) related to the mountain belt elongation (Fig. 7) emphasize the northwards direction of the Arabian plate motion.

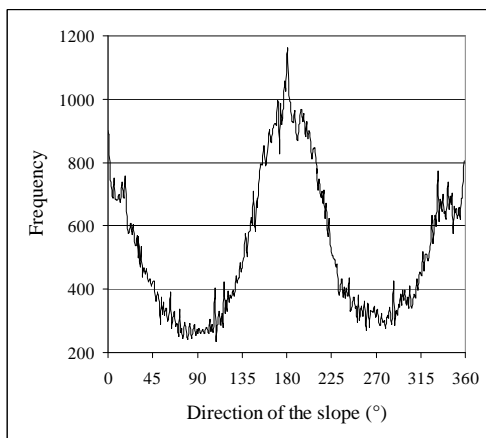


Figure 7 Aspect of the mountain belt.

Figures 8 and 9 illustrate the results obtained by means of such a procedure. The treatment stops when the coastal line is more or less linear. It is then possible to calculate the rate motion of the moving lithospheric plate.

Moreover, the roughness of a profile provides information about the end result of the treatment. It is well known that the Hurst exponent  $\zeta \neq 1$  applied to an auto-related fractal represents a reliable technique to analyze the roughness of a

profile by means of moving window according to the rescaling  $x \rightarrow \gamma x$  and  $y \rightarrow \gamma^\zeta y$ .

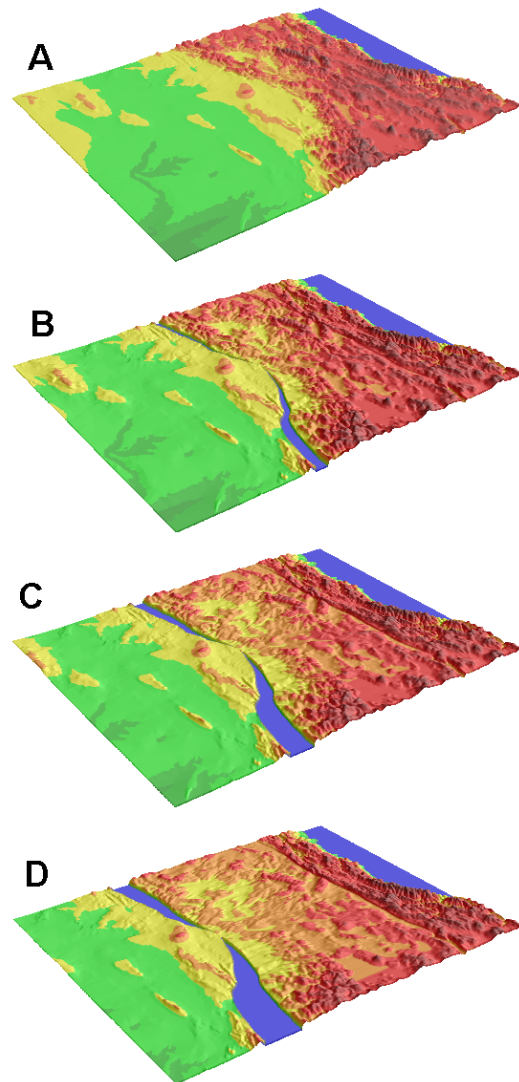


Figure 8 Punching motion.

The Hurst exponent of the cross sections reported in figure 9 increases regularly (Fig. 10). Our results indicate that the profile roughness decreasing is closely related to the stretching applied here and confirms the validity of the treatment.

## CONCLUSION

The developed algorithm allows simulating the effect of a plate collision in order to reconstruct the former landscape of the obducted plate. This relevant treatment permits defining the moment when the mountain belt disappears and the costal line is quite linear, allowing to calculate the motion rate of the moving lithospheric plate. In the

Parrot and Collet, Simulation of lithospheric-plate collision by using DEM. Example of the Arabian platform motion.

case of Eastern Turkey, the total displacement measured is equal to 210 km. Thus the rate motion of the Arabian plate corresponds to 10.5 mm/year if we assumed that the movement began 20 million years before present (Burdigalian) or to 8.9 mm/year for 23.5 million years (Aquitainian).

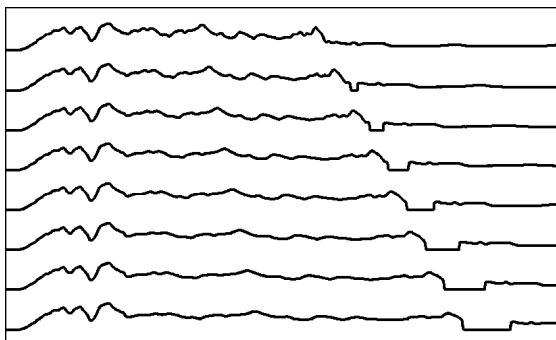


Figure 9 Cross sections.

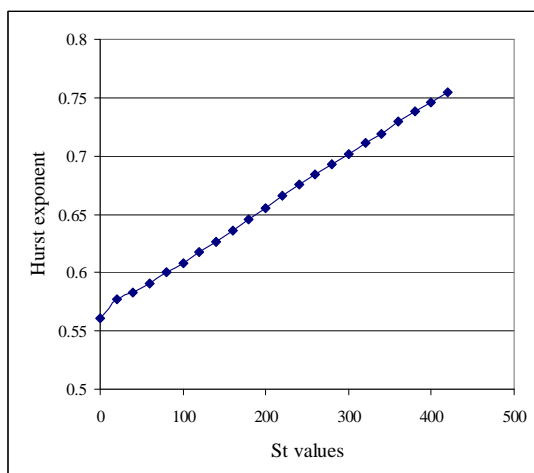


Figure 10. Evolution of the Hurst exponent according to the St increasing.

## References

- Bartsch, K. P., Van Miegroet, H., Buettinger, J., Dobrowski, P. (2002). Using empirical erosion models and GIS to determine erosion risk at cap Willians, Utah. *Journal of Soil and Water Conservation* 57 (1): 29-37.
- Calixto-Albarran, I., Parrot, J.F. (2007). Reconstrucción del Fondo del embalse de La Vega (México) y su evolución mediante MDT y datos de satélite. Congreso Geomática, Barcelona, Febrero 2007, 10 p.
- England, P., Houseman, G. (1986). Finite strain calculations of continental deformation: 2. Comparison with the India-Asia collision zone, *J. Geophys. Res.*, 91, 3664–3676.
- Gao, Q, L., Ci, Yu, N. (2002). Modeling wind and water erosion in northern China under climate and land use changes. *Journal of Soil and Water Conservation* 57 (1): 47-55.
- Houseman, G., England, P. (1993), Crustal thickening versus lateral expulsion in the India-Asian continental collision, *J. Geophys. Res.*, 98, 12,233–12,249.
- Lee, J.J., Phillips, D.L., Benson, V.W. (1999). Soil erosion and climate change: Assessing potential impacts and adaptation practices. *Journal of Soil and Water Conservation* 54 (3): 473-476.
- Peltzer, G., Saucier, F. (1996), Present-day kinematics of Asia derived from geological fault rates, *J. Geophys. Res.*, 101, 27,943–27,956.
- Peltzer, G., Tapponnier, P. (1998), Formation and evolution of strikeslip faults, rifts, and basins during the India-Asia collision: An experimental approach, *J. Geophys. Res.*, 103, 15,085–15,117.
- Sengor, A., Özeren, S., Genç, T., Zor, E. (2003) East Anatolian high plateau as a mantle supported, north-south shortened domal structure. *Geophysical Research Letters*, 30(24), 1-12.
- Tapponnier, P., Peltzer, G., Le Dain, A.Y., Armijo, R., Cobbold, P. (1982), Propagating extrusion tectonics in Asia: New insights from simple experiments with plasticine, *Geology*, 10, 611–616.
- Thatcher, W. (2003). GPS constraints on the kinematics of continental deformation, *Int. Geol. Rev.*, 45, 191–212.
- Watson, A., Evans, R. (1991). A comparison of estimates of soil erosion made in the field and from photographs. *Soil and Tillage Research* 19: 1727-1735.
- Wilson, J.P., Gallant, J.C. (2000). *Terrain Analysis. Principles and Applications*. John Willey & Sons, New York, 479 pp.